Cerebral Cortex April 2007;17:935-941
doi:10.1093/cercor/bhl004
Advance Access publication June 1, 2006

Neurons in V1 Patch Columns Project to V2 Thin Stripes

Lawrence C. Sincich, Cristina M. Jocson and Jonathan C. Horton

Beckman Vision Center, University of California—San Francisco, San Francisco, CA 94143, USA

In the primate, connections between primary visual cortex (V1) and the second visual area (V2) are segregated according to the characteristic pattern of cytochrome oxidase (CO) activity in each of these cortical areas. Patches supply thin stripes, whereas interpatches supply pale stripes and thick stripes. Previously, the projection from patches to thin stripes was reported to arise exclusively from layer 2/3. In this present report, we made injections of a retrograde tracer, cholera toxin-B (CTB-Au), into macaque V2 thin stripes to re-examine the laminar origin of their input from V1. While the great majority of cells indeed resided in layer 2/3, small populations were also present in layers 4A, 4B, and 5/6. The location of CTB-filled cells in each layer was analyzed to determine the relationship with CO patches. Cells in layers 2/3, 4A, and 4B were aggregated into patches, forming columns that project to thin stripes. Surprisingly, cells in layer 5/6 were scattered, seemingly at random. These findings confirm that the main V1 projection to V2 stripes emanates from patches in layer 2/3. However, multiple V1 layers innervate V2 thin stripes, and the projection from layer 5/6 does not respect the patch/interpatch dichotomy.

Keywords: cholera toxin, color vision, column, cytochrome oxidase, flatmount, visual cortex

Introduction

The second visual area (V2) in the macaque brain receives input from perhaps a dozen different cortical areas (Kennedy and Bullier 1985; Stepniewska and Kaas 1996; Gattass and others 1997). The dominant projection is provided by the primary visual cortex (V1). After injection of a retrograde tracer in V2, about two-thirds of the cells labeled throughout the entire cerebral cortex are located in V1 (Sincich and others 2003). This result means that the "feedforward" projection from V1 to V2 is twice as strong, at least in numeric terms, as the entire "feedback" projection to V2 from higher cortical areas. To determine the function of V2, it is vital to have an accurate anatomical description of the input it receives from V1.

The original studies concerning the links between cytochrome oxidase (CO) compartments in V1 and V2 reported a segregated tripartite system of projections (Livingstone and Hubel 1984, 1987). Importantly, the cells projecting to each class of V2 stripe were found to arise from a single layer in V1. Layer 2/3 was identified as the source of input to the pale and thin stripes, whereas layer 4B was determined to supply only the thick stripes (Fig. 1). From a functional standpoint, this discovery meant that each V2 stripe class appeared to receive input from an entirely different V1 compartment: layer 2/3 patches → thin stripes, layer 2/3 interpatches → pale stripes, layer 4B patches and interpatches → thick stripes. Anatomical isolation of each projection stream provided perhaps the most compelling evidence in support of the proposal of Livingstone and Hubel (1988) that thin, pale, and thick stripes are specialized for different visual attributes.

A re-examination of the projections from V1 to V2 has revealed a pattern of connections that differs from the account of Livingstone and Hubel (1984, 1987) in several key respects (Sincich and Horton 2002). First, layer 2/3 sends a strong projection to all 3 V2 stripe classes. Second, interpatches innervate both pale stripes and thick stripes. Consequently, the V1 projection to V2 is bipartite rather than tripartite because pale and thick stripes get their input from the same V1 compartment. Third, layer 4B projects weakly to all 3 types of V2 stripes. Fourth, layers 4A, 5, and 6 also supply V2 stripes.

Recently, we performed a quantitative analysis of the V1 to V2 projection, focusing on the thin stripes (Sincich and Horton 2005a). CO activity in layer 2/3 in V1 was thresholded to define objectively the borders of CO patches. The location of each labeled cell was then plotted to determine the percentage of cells located in patches. We confirmed that the input to thin stripes is confined largely to patches (Livingstone and Hubel 1984; Sincich and Horton 2002). In this study, the distribution of labeled cells was plotted only in layer 2/3. We have now examined the distribution of labeled cells in the remaining cortical layers. The goals of this new analysis were to determine the relative numerical strength of the projection to thin stripes provided by each layer of V1 and whether this projection is derived from CO patches for each layer of V1.

Methods

Experimental Animals

Experiments were performed in 17 normal adult macaques weighing 6–10 kg, following procedures described in detail elsewhere (Sincich and Horton 2002, 2005a). In brief, a half-dozen pressure injections of 0.1% gold-conjugated cholera toxin-B subunit (CTB-Au from List Biological, Campbell, CA) (Llewellyn-Smith and others 1990) were made along the edge of the lunate sulcus in V2 in each hemisphere. This sliver of exposed V2 represents the visual field near the lower vertical meridian. It is possible that injections made within the lunate sulcus might have yielded different results, but this seems doubtful because V1 to V2 projections are unlikely to vary according to polar angle in the visual field. All injections were made at a depth of 1 mm to center the injection site in layer 4. This layer receives the bulk of V1 input; we did not test whether varying the depth of the V2 tracer injection might affect the proportion of labeled cells in different V1 layers. After 2–3 days for transport, animals were euthanized with pentobarbital (150 mg/kg) and perfused with normal saline followed by 1 L of 1% paraformaldehyde in 0.1 M phosphate buffer, pH 7.4. Flatmounts containing V1 and V2 (Sincich and others 2003) were cut tangentially at 50 μm, dried on slides, and processed for CO (Wong-Riley 1979). The sections were then double-labeled by silver intensification of the CTB-Au with an IntenSE-M kit (Amersham, Little Chalfont, UK). In some monkeys, paired tracer

injections were made of CTB-Au and wheat germ agglutinin conjugated to horseradish peroxidase (WGA-HRP). In these animals, alternate sections were processed either for CO and CTB-Au or for CTB-Au and WGA-HRP.

Data Analysis

Tracer injections were made blindly in V2 with respect to stripe type. Only 77/187 injections landed within a stripe of clear identity. The remaining injections were rejected for analysis because they spread into an adjacent stripe, strayed across the border into V1, were too small for detectable transport, or were situated in a stripe of uncertain type. Of the 77 usable injections, 17 were located in thin stripes. In all 17 cases, labeled cells in V1 were concentrated in patches. In a previous report, this relationship was shown by thresholding the density of silver grains at low power to define contours of label intensity, which coincided with the CO patches (Sincich and Horton 2002). In a later study, we plotted the position of each CTB-Au–filled cell in layer 2/3 for 8/17 cases (Sincich and Horton 2005a). The injection sites for these 8 cases are available at: http://www.jneurosci.org/cgi/content/full/25/44/10087/DC1. These cases were picked because the CTB-Au injection landed in the core of a thin strip, minimizing spillover into adjacent pale stripes. Such cases tend to show the most discrete patch labeling in V1.

In this present study, we analyzed the location of cells outside layer 2/3 for these 8 exemplary cases. Serial sections from the pia to the white matter were inspected in the microscope using brightfield illumination to visualize CO and darkfield/crossed Polaroid filters to detect CTB-Au–filled cells. In most cases, tissue sections were double-labeled for CO and CTB-Au. This made it easy to assign labeled cells to their cortical layer, based on the characteristic laminar pattern of CO staining (Horton 1984). In all 8 cases, we plotted the location of labeled cells in a single section passing through layer 4B. For a single case, we also plotted the location of labeled cells in layers 4A. For 2 cases, we plotted all the labeled cells in layer 5/6. For the remaining cases, the distribution of labeled cells in layers 4A, 5, and 6 was ascertained by visual inspection.

The location of CTB-Au–labeled cells was plotted with a camera lucida attachment at ×200 magnification. Data were entered into a computer using a Wacom Cintiq 15× LCD tablet in conjunction with AutoCAD 2002 software. To quantify the CO staining, photographs were taken with a Spot RT color CCD camera mounted on an Olympus SZH10 microscope. Vessel profiles were filled in with pixels of the mean gray level value of the image using Photoshop 7.0. To correct for global changes in section density, a low-pass Fourier-filtered (cutoff frequency = 1.1 cycles/mm) image was subtracted from the original image using Matlab. The resulting image was then blurred with a Gaussian filter (σ = 45 μm) and divided into 6 zones of equal area based on the density of CO staining. The darkest 2 zones (33% area) were designated as patches; the palest 4 zones were defined as interpatches (66% area) (Horton 1984; Purves and LaMantia 1993; Farias and others 1997; Sincich and Horton 2003).

Results

Figure 2 shows a CTB-Au injection in a thin stripe. The injection in V2 produced a field of cells labeled by the retrograde tracer at the expected, corresponding retinotopic location in V1. The overwhelming majority of labeled cells were present in layer 2/3. Figure 3*a* shows the most densely labeled section, which passed through layer 3. There were 3831 filled cells in this field, grouped into about 30 clusters. Examination of the same section in brightfield illumination revealed the CO patches (Fig. 3*b*). The density of CO activity was divided into 6 zones of equal area; the darkest 2 represented patches (Fig. 3*c*). A plot of each labeled cell superimposed onto the contours of CO density showed that most cells (64%) were situated in patches (Fig. 3*d*). Overall, a mean of 81% of cells in the 8 quantified cases was located in patches (Sincich and Horton 2005a). The case illustrated in Figure 3 showed the weakest tendency among the 8 cases for labeled cells to aggregate into patches, perhaps because the tracer injection extended slightly into the pale stripes flanking the thin stripe. The percentage of cells located in patches depends, of course, on the criterion used to define a patch. If one assigns more than a third of the cortex to patches, the proportion of cells located within patches will increase. The important point is that the fields of cells centered on CO patches project to thin stripes; they show little overlap with fields of cells in interpatches that project to pale stripes (Sincich and Horton 2005a).

Figure 4 shows the same field, 100 μm deeper, passing through layer 4A. Too few CTB-Au–filled cells were present in layer 4A to be discernable in a photograph at low power. Another case has been published elsewhere, showing visible patches of labeled cells in 4A after a thin stripe injection (Sincich and Horton 2002, see Supplementary Fig. 1*B*). Labeled cells were located in the pale interstices of the honeycomb-like

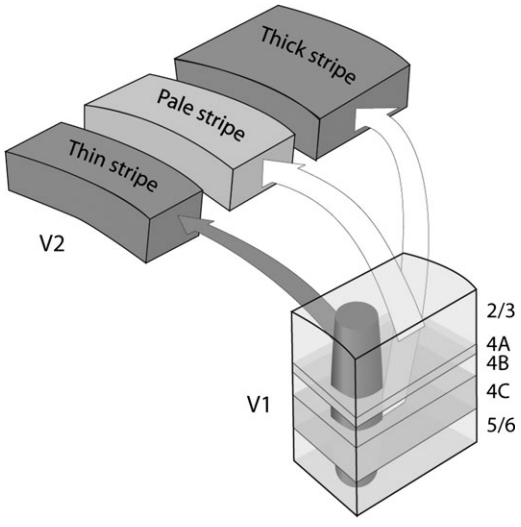

Figure 1. Pattern of projections from V1 to V2, according to Livingstone and Hubel (1984, 1987). The input to each V2 stripe is supplied by a single V1 source: layer 2/3 patches → thin stripes; layer 2/3 interpatches → pale stripes; layer 4B → thick stripes.

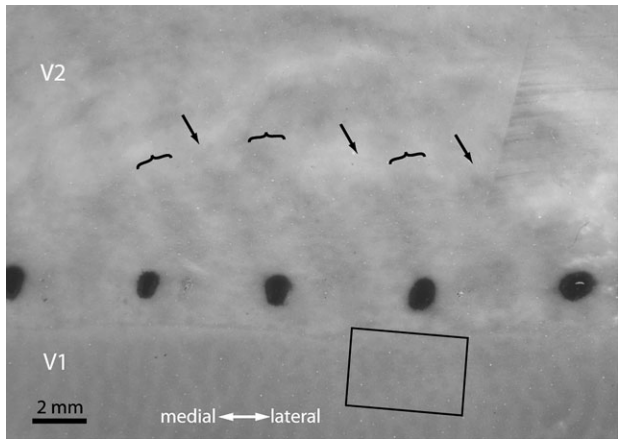

Figure 2. CO section from a flatmount of the right hemisphere, showing a string of CTB-Au injections in V2. Alternating thin (arrows) and thick stripes (brackets) are visible. The rectangular box contains the field of retrogradely labeled cells, analyzed for different layers in subsequent figures. In this section, the box grazes the border between 4B and 4Cα. Ocular dominance columns are visible in layer 4C because one eye was enucleated 3 days before perfusion, in connection with an unrelated experiment.

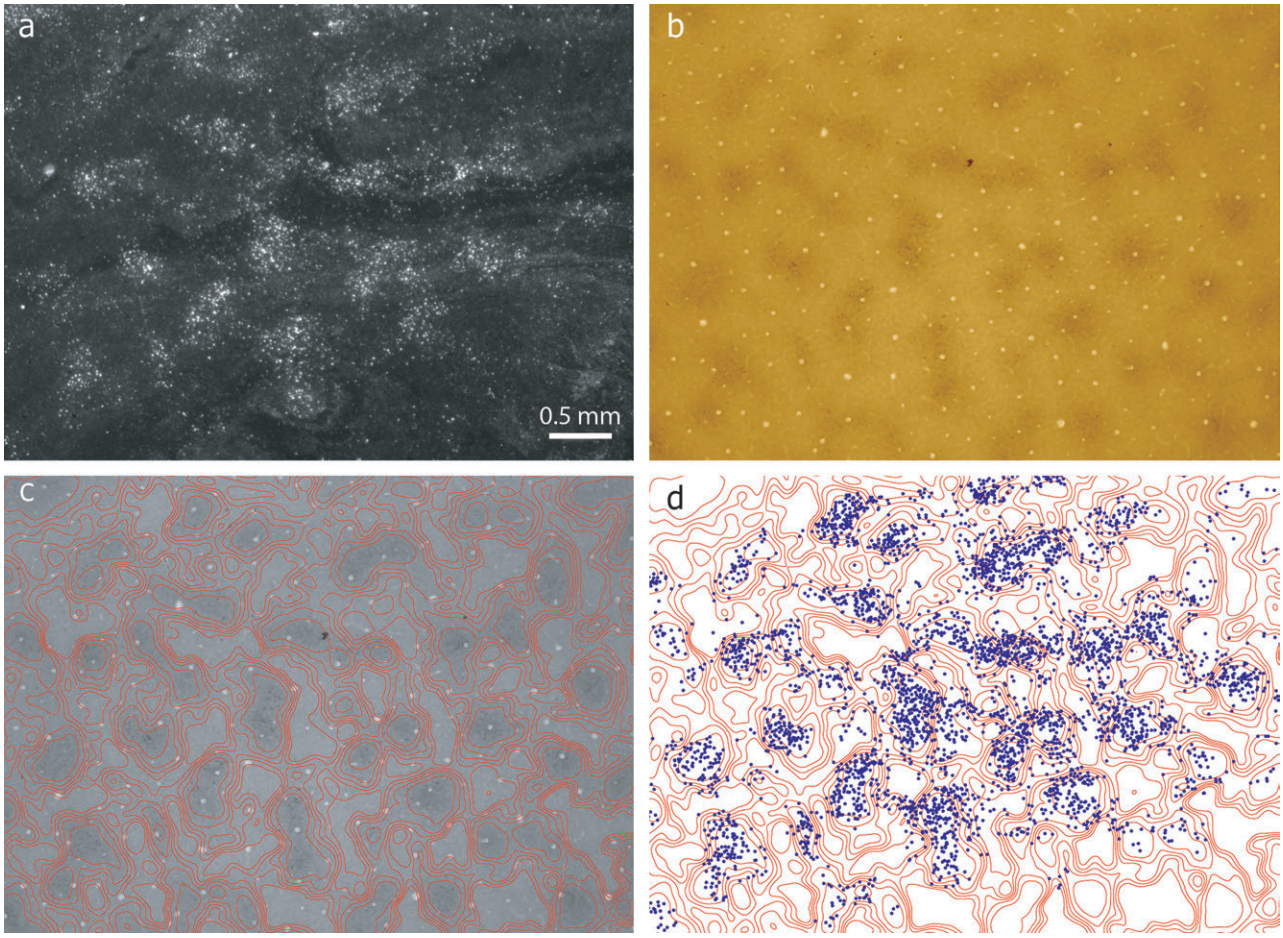

Figure 3. Cell labeling in layer 3. (*a*) This darkfield image from a section 200 μm superficial to the section in Figure 2 shows clusters of CTB-Au–filled cells. The field is from the boxed region in Figure 2. (*b*) The same section, now viewed in brightfield, shows the CO patches. (*c*) Density contours, dividing the section into 6 zones of equal area based on the intensity of CO activity. (*d*) Alignment of cells (blue dots) and patches, shown by superimposing the position of each CTB-Au–filled cell on the CO contours.

CO pattern, corresponding to the pyramidal cell modules identified by Peters (1994). Altogether, 157 CTB-Au–filled cells could be identified at high power, corresponding to 4% of the density of labeled cells in the layer 2/3 section (Fig. 4*b*). Their location with respect to the patches is plotted in Figure 4*c*. Most cells (63%) were located in register with patches (Fig. 4*d*). A 2-way χ^2 test revealed that cells were significantly more likely to be located in register with patches than interpatches ($P < 10^{-6}$). Examination of layer 4A in the other 7 cases confirmed that labeled cells were located preferentially in patch columns.

Figure 5*a* shows the distribution of labeled cells in layer 4B for the same V2 injection. This tissue section was processed free-floating for CTB-Au and WGA-HRP. In general, free-floating, wet sections show stronger silver intensification than slide-mounted, previously dried sections. This explains, in part, the visibility of the relatively scant cell labeling in this section. It was not processed for CO, so adjacent sections had to be inspected to determine its cortical layer. The section 50 μm more superficial (Fig. 4*a*) passed through layer 4A. The section 50 μm deeper (Fig. 5*b*) straddled the border between 4B and 4Cα. Therefore, the section shown in Figure 5*a* could be assigned reliably to layer 4B.

Altogether, there were 362 labeled cells in the layer 4B field, or about 9% of the density of labeled cells present in the layer 2/3 field (compare Fig. 3*a* and 5*a*). CO patches are faint in layer 4B. Therefore, the contours of the CO patches in the layer 2/3 section were transferred onto the plot of labeled cells in layer 4B, using blood vessels for alignment (Fig. 5*c*). The labeled cells clustered preferentially in patches (Fig. 5*d*), with 68% of cells in the darkest 2 zones of CO staining.

A mixture of small pyramidal cells and stellate cells was labeled in layer 4B after tracer injection into thin stripes (Fig. 5*e*). The location of every labeled cell in layer 4B was plotted for all 8 cases (see Supplementary Table). Overall, 74% of labeled cells were located in CO patches (Fig. 5*f*). Cells were significantly more likely to be located in patches than interpatches (χ^2 test, $P < 10^{-10}$). Although the aggregation of cells into patches for the 8 injections seemed less marked in layer 4B (74%) than in layer 2/3 (81%), this difference was not significant (Wilcoxon rank sum test, $P = 0.29$).

Layers 5 and 6 contained a smattering of CTB-Au–labeled cells (Fig. 6). About 15% were large pyramidal cells that had the typical appearance of Meynert cells (Fig. 6*c*) (Payne and Peters 1989). Retrogradely labeled cells were not confined to a narrow tier in layers 5 and 6, but were scattered throughout the depth of these layers. The location of labeled cells in 5 serial sections, containing all of layers 5 and 6, is shown in Figure 6*b*. There were 154 cells, 37% located in patches. Cells in layer 5 and 6 were not preferentially clustered into patches (χ^2 test, $P = 0.23$). To confirm this result, the cells in layer 5/6

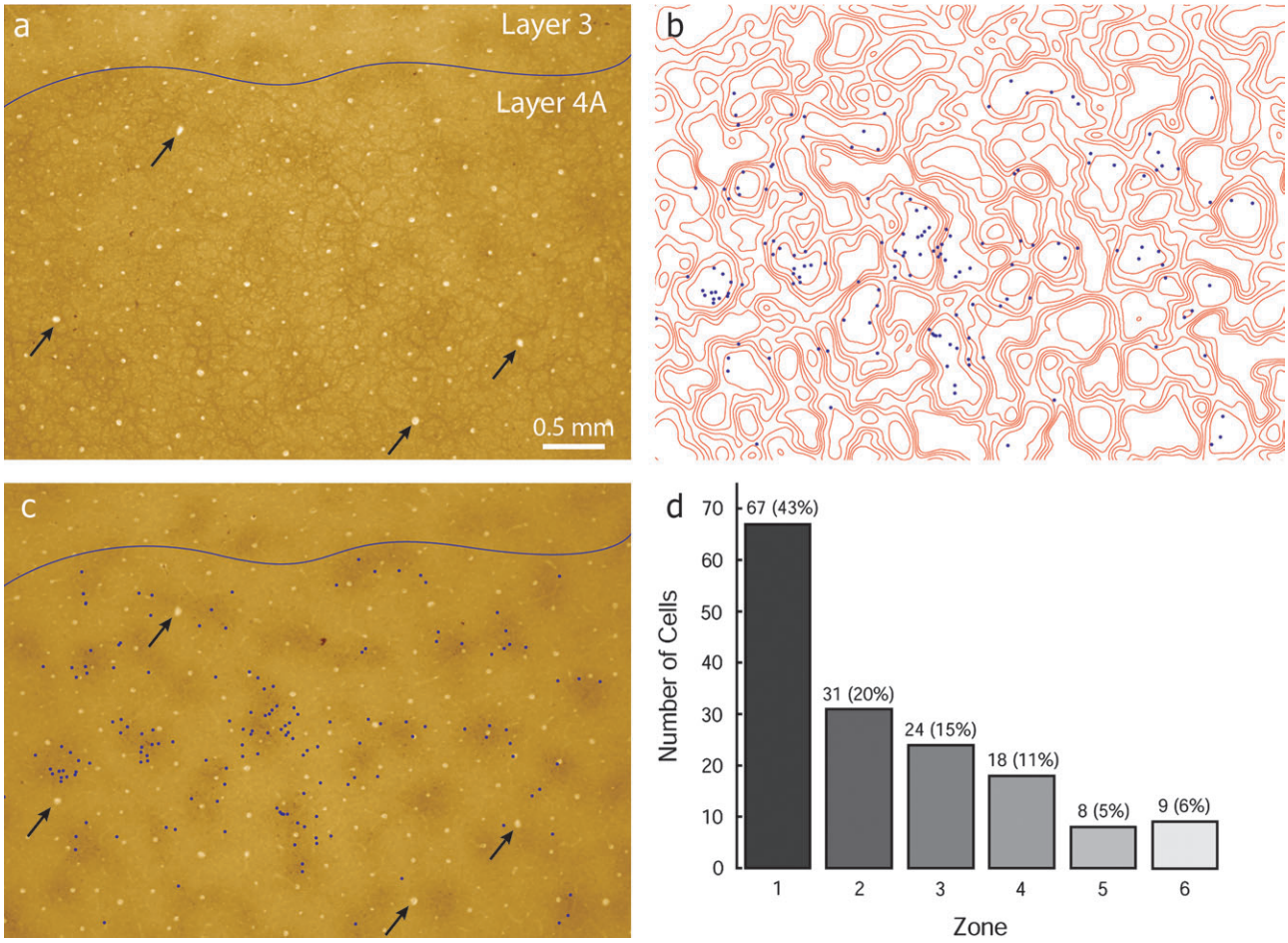

Figure 4. Cell labeling in layer 4A. (*a*) Same field as in Figure 3, from a section 100 μm deeper, showing the characteristic "honeycomb" CO pattern in layer 4A. (*b*) Alignment of cells and patches in layer 4A. Because patches are not visible in layer 4A, contour lines were transferred from Figure 3c. (*c*) Superimposition of labeled cells in 4A on CO section from layer 2/3, to show that 4A cells projecting to thin stripes were clustered in patches. Arrows denote blood vessels used for alignment. (*d*) Histogram showing that 63% of labeled cells were located in the 2 darkest zones of CO staining.

were plotted for a second case, injection 6. There was a total of 224 cells, with 79 (35%) located in patches. Once again, there was no tendency for labeled cells to aggregate within patches (χ^2 test, $P = 0.47$).

Discussion

Livingstone and Hubel (1984) reported that V1 input to each CO stripe class is provided by a single layer: 2/3 → thin stripes and pale stripes and 4B → thick stripes. They found no evidence for V1 to V2 projections emanating from other cortical layers. However, other investigators subsequently identified labeled cells in layers 4A, 5, and 6, in addition to layers 2/3 and 4B, after injection of retrograde tracers into V2 (Kennedy and Bullier 1985; Van Essen and others 1986; Cusick and Kaas 1988; Rockland 1992; Levitt and others 1994). The functional meaning of this multi-layered input from V1 to V2 stripes is addressed more fully elsewhere (Sincich and Horton 2005b). In this present study, our goal has been to quantify the relative strength of the projection to V2 thin stripes arising from each cortical layer. In addition, we have determined how the projection coming from each layer is organized with respect to the CO patches. We have done this by plotting cells in tangential sections from pia to white matter and comparing their distribution with the density of CO activity. No prior study has used this approach to provide a description of the relative numerical strength, as a function of both cortical layer and column, for a projection from one area to another.

After CTB-Au tracer injection into 8 thin stripes, we detected retrogradely labeled cells in layers 2, 3, 4A, 4B, 5, and 6 of V1 in every case. In one example, the numerical strength of the projection from each layer was compared by counting labeled cells in multiple sections. The projection from layer 3 (3831 cells) was far richer than the projection from layer 4A (157 cells), layer 4B (362 cells), or layer 5/6 (154 cells). These cell counts actually understate the predominance of the contribution from layer 2/3 because they neglect the relative thickness of different cortical layers. In this particular case, 20 tissue sections 50- μm thick were obtained from pia to white matter (the cortex is thicker in vivo, but it shrinks to only ~1 mm after fixation and flat mounting). Layer 2/3 was contained in sections 2–7; the count of 3831 cells was obtained from section 6. Section 2 was lightly labeled, but sections 3–7 showed about the same number of labeled cells as section 6. Thus, one can estimate that layer 2/3 contained 19,155 cells (5 × 3831) labeled by the tracer injection. Layer 4A was confined to section 8 (157 cells). Layer 4B occupied section 9 (362 cells) and about half section 10, yielding an estimated 4B cell tally of 543

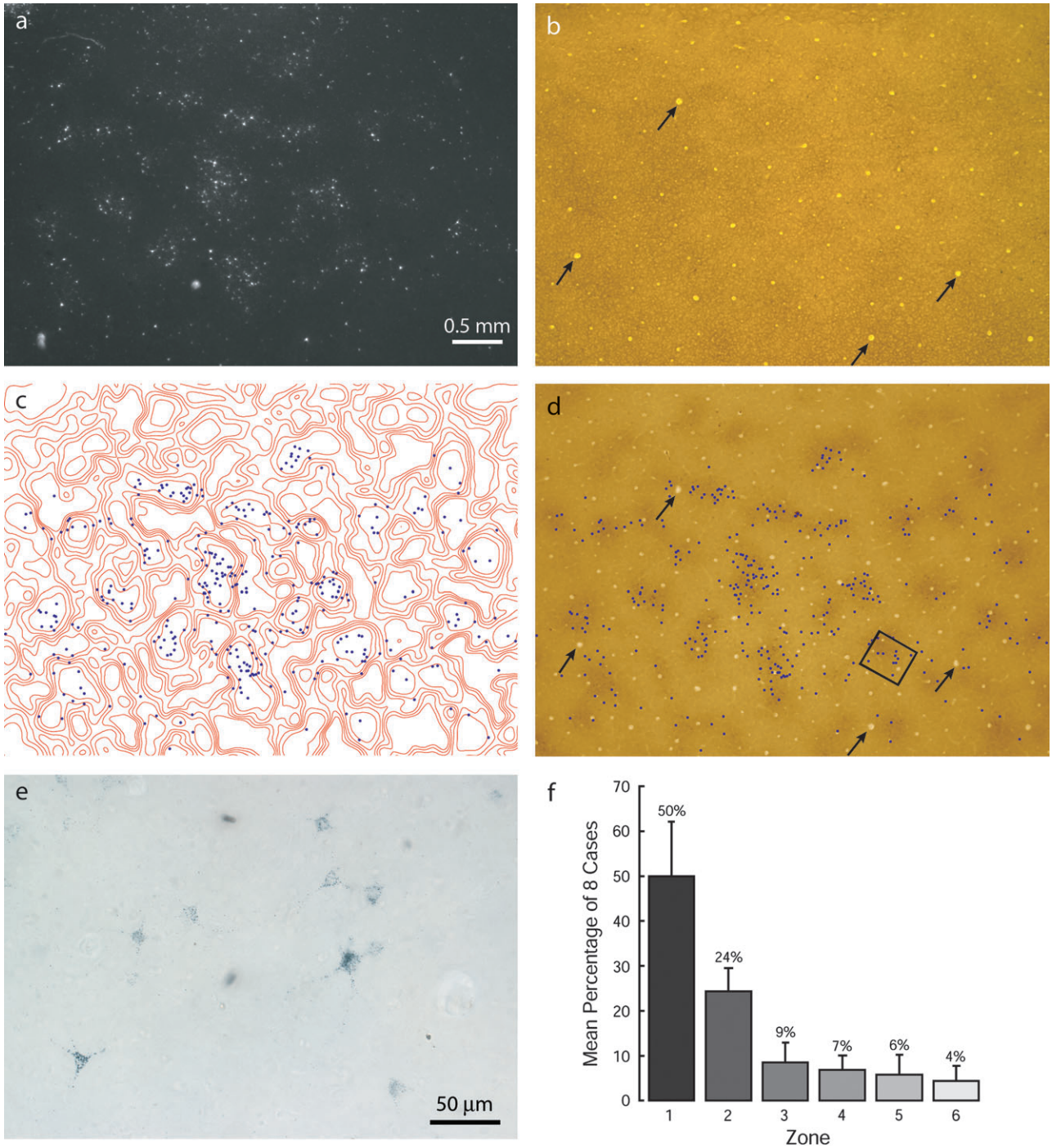

Figure 5. Cell labeling in layer 4B. (*a*) Same field as in Figure 3, from a section 150 µm deeper, showing clusters of labeled cells in darkfield. (*b*) Adjacent CO section, 50 µm deeper, at the layer 4B/4Cα border. (*c*) Labeled cells in 4B superimposed on contours of CO density from Figure 3*d*. (*d*) Labeled cells in 4B superimposed on the CO-staining pattern in Figure 3*b*. (*e*) Magnified view of the box in (*d*) showing CTB-Au–filled cells in a CO patch. (*f*) Histogram from all 8 cases, showing that a mean percentage of 74% of layer 4B cells was located in CO patches.

(1.5 × 362). Layer 4C filled sections 11–15. Collectively, sections 16–20 yielded 154 cells in layers 5 and 6. Taking into account these adjustments, the relative projection strengths from each layer were 2/3 (95%), 4A (1%), 4B (3%), and 5/6 (1%). This is only an estimate because we have not actually counted all the cells in layer 2/3, and extrapolation from a single section would require an Abercrombie correction (Guillery and August 2002). Nonetheless, layer 2/3 clearly provides the vast majority of cellular projections to thin stripes.

The proportion of projection neurons arising from the supragranular versus infragranular layers has been used to infer whether a projection is feedforward or feedbackward (Kennedy and Bullier 1985; Felleman and Van Essen 1991; Barone and others 2000). The fact that 95% of cells in V1 projecting to V2 thin stripes arise from layer 2/3 indicates that the projection is feedforward. The density of cells projecting from V1 to V2 thin stripes is difficult to determine because the number of retrogradely filled cells varies depends on the choice of tracer,

injection size, histological processing, etc. Among our 8 CTB-Au injections, there was a 5-fold variation in the number of labeled cells in layer 2/3 and even greater variation in layer 4B. Injection 3 yielded the most labeled cells in layers 2/3 and 4B (Sincich and Horton 2005a). Within the central 5 mm^2 of the field of labeled cells, where cell density peaked, there were 1054 labeled cells/mm^2 in a single section of layer 2/3 and 44 cells/mm^2 in the same region of layer 4B. Extrapolating through the depth of the cortex, this corresponds to 5380 V1 cells/mm^2 that project to V2 thin stripes. Correcting for the proportion of these cells located in patches, and the fraction (1/3) of cortex representing patches, there was a patch projection density of 13,070 cells/mm^2. This figure, which represents about 7% of the cells beneath the surface of each mm^2 of V1, is close to Rockland's (1997) mean figure (14,000 cells/mm^2) for the density of V1 cells projecting to V2. Given a density of about 4 patches/mm^2 in this example, there were an average of 3270 V1 → V2 projection cells per patch through all cortical layers.

Given that so few labeled cells were found in layer 4B after thin stripe injections, it is legitimate to inquire if they might have occurred from tracer spillover into pale or thick stripes, which are known to be recipients of 4B input (Livingstone and Hubel 1987; Sincich and Horton 2002). The strongest argument against this idea is that the 4B input to pale stripes and thick stripes is supplied by interpatches (Sincich and Horton 2002). In contrast, the 4B labeling seen after thin stripe injections in our experiments was concentrated in patches. It was thus likely to represent a genuine layer 4B input to thin stripes. The same was true for the labeling in layer 4A.

Although the supragranular projection to thin stripes arose predominately from patches, the projection from layer 5/6 showed no such predilection. This difference in compartmentalization suggests that the infragranular projection serves a different function. Labeled cells were scattered sparsely in both patches and interpatches (Fig. 6). Meynert cells tend to be situated outside CO patches (Fries 1986; Payne and Peters 1989). Because Meynert cells were present among the layer 5/6 population filled by thin stripe injections, they would tend to nullify any correlation between labeled cells in layer 5/6 and patches. In addition, Meynert cell axon collaterals make widespread, patchy connections within layer 6 of V1 (Li and others 2003). If Meynert cell axons show the same behavior in V2, they would be likely to innervate more than one stripe class. This might also account for their diffuse distribution in layer 5/6 after thin stripe tracer injections. It would be valuable to learn how axons from cells from different layers and compartments of V1 ramify in V2. Reconstruction of individual V1 fibers has shown that they terminate in multiple clusters, separated by 200–500 μm, in layers 3 and 4 of V2, with minor projections to layer 5 (Rockland and Virga 1990). However, correlation with different CO compartments and cortical layers has not been performed.

The results from our analysis support the basic conclusion of Livingstone and Hubel (1984) that the main V1 input to V2 thin stripes is from patches in layer 2/3. We add here the observation that minor inputs also arise from layers 4A, 4B, and 5/6 (Fig. 7).

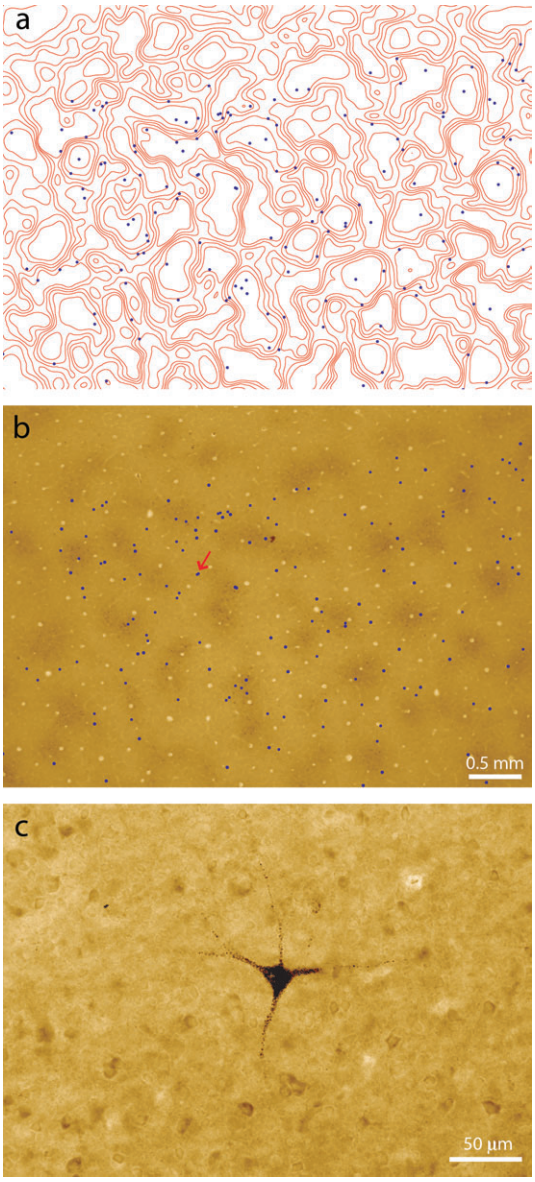

Figure 6. Cell labeling in layers 5 and 6. (*a*) Position of cells in 5 serial sections plotted on contours of CO density from layer 2/3. (*b*) Position of cells plotted directly on pattern of CO activity from layer 2/3. The cells are not located preferentially in patches. (*c*) A Meynert cell filled with CTB-Au in layer 6. Its location is marked with a red arrow in (*b*).

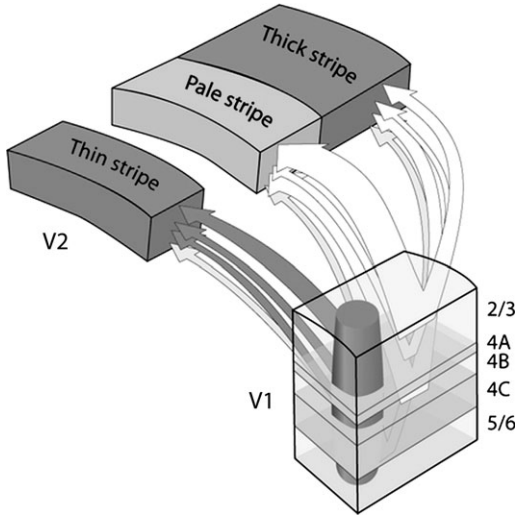

Figure 7. Summary of V1 to V2 projections. For all stripes the strongest input comes from layer 2/3, but 4A, 4B, and 5/6 also contribute. The input is dichotomized: patches → thin stripes; interpatches → pale, thick stripes, except from layer 5/6.

The largest projection outside layer 2/3 is contributed by 4B. It has been proposed that thin stripes are specialized for color processing (Livingstone and Hubel 1988; Roe and Ts'o 1997). If so, it is not clear what function is served by the projection from 4B, a layer strongly influenced by the magno pathway (Yabuta and others 2001). Perhaps the cells in patches that project to thin stripes have unique properties that do not conform to the dominant magno character of layer 4B. It is also possible that thin stripes fulfill other functions, besides color perception (Gegenfurtner and Kiper 2003), and that these functions require magno input. In this context, it is probably not accurate to use the terms "thin stripe" and "color stripe" synonymously.

Previously, it was emphasized that layer 4B projects exclusively to thick stripes and that thick stripes receive their input exclusively from 4B (Fig. 1) (Livingstone and Hubel 1987). This concept was invoked to explain why thick stripes should be specialized for motion and stereo processing. These functions were thought to depend heavily on signals conveyed by the magno laminae of the lateral geniculate nucleus. It is now apparent that layer 4B projects all V2 stripes: thin, pale, and thick. The 4B projection to thin stripes is more sparse than the 4B projection to pale and thick stripes (Sincich and Horton 2002). However, a more noteworthy consideration is that the 4B input is minor, "for all 3 V2 stripe types", compared with the layer 2/3 input. Thus, it is likely that differences in the signals transmitted by layer 2/3 to thin, pale, and thick stripes have the strongest impact on functional specialization. Future studies should be directed at uncovering the properties of these major projections. At this point, we know only that they are divided by CO, with patches supplying thin stripes and interpatches feeding pale and thick stripes (Fig. 7).

Supplementary Material

Supplementary material can be found at: http://www.cercor.oxfordjournals.org/.

Notes

This work was supported by grants EY10217 (JCH), EY13676 (LCS), and EY02162 (Beckman Vision Center) from the National Eye Institute. The California Regional Primate Research Center is supported by National Institutes of Health Base Grant RR00169. Amar Marathe assisted with data analysis, and Robin Troyer provided animal care. *Conflict of Interest*: None declared.

Address correspondence to Jonathan C. Horton, MD, PhD, Beckman Vision Center, University of California—San Francisco, 10 Koret Way, San Francisco, CA 94143-0730, USA. Email: hortonj@vision.ucsf.edu.

References

Barone P, Batardiere A, Knoblauch K, Kennedy H. 2000. Laminar distribution of neurons in extrastriate areas projecting to visual areas V1 and V4 correlates with the hierarchical rank and indicates the operation of a distance rule. J Neurosci 20:3263–3281.

Cusick CG, Kaas JH. 1988. Cortical connections of area 18 and dorsolateral visual cortex in squirrel monkeys. Vis Neurosci 1:211–237.

Farias MF, Gattass R, Piñón MC, Ungerleider LG. 1997. Tangential distribution of cytochrome oxidase-rich blobs in the primary visual cortex of macaque monkeys. J Comp Neurol 386:217–228.

Felleman DJ, Van Essen DC. 1991. Distributed hierarchical processing in the primate cerebral cortex. Cereb Cortex 1:1–47.

Fries W. 1986. Distribution of Meynert cells in primate striate cortex. Spatial relationship with cytochrome oxidase blobs. Naturwissenschaften 73:557–558.

Gattass R, Sousa AP, Mishkin M, Ungerleider LG. 1997. Cortical projections of area V2 in the macaque. Cereb Cortex 7:110–129.

Gegenfurtner KR, Kiper DC. 2003. Color vision. Annu Rev Neurosci 26:181–206.

Guillery RW, August BK. 2002. Doubt and certainty in counting. Prog Brain Res 135:25–42.

Horton JC. 1984. Cytochrome oxidase patches: a new cytoarchitectonic feature of monkey visual cortex. Philos Trans R Soc Lond B Biol Sci 304:199–253.

Kennedy H, Bullier J. 1985. A double-labeling investigation of the afferent connectivity to cortical areas V1 and V2 of the macaque monkey. J Neurosci 5:2815–2830.

Levitt JB, Yoshioka T, Lund JS. 1994. Intrinsic cortical connections in macaque visual area V2: evidence for interaction between different functional streams. J Comp Neurol 342:551–570.

Li H, Fukuda M, Tanifuji M, Rockland KS. 2003. Intrinsic collaterals of layer 6 Meynert cells and functional columns in primate V1. Neuroscience 120:1061–1069.

Livingstone MS, Hubel DH. 1984. Anatomy and physiology of a color system in the primate visual cortex. J Neurosci 4:309–356.

Livingstone MS, Hubel DH. 1987. Connections between layer 4B of area 17 and the thick cytochrome oxidase stripes of area 18 in the squirrel monkey. J Neurosci 7:3371–3377.

Livingstone MS, Hubel DH. 1988. Segregation of form, color, movement, and depth: anatomy, physiology, and perception. Science 240:740–749.

Llewellyn-Smith IJ, Minson JB, Wright AP, Hodgson AJ. 1990. Cholera toxin B-gold, a retrograde tracer that can be used in light and electron microscopic immunocytochemical studies. J Comp Neurol 294:179–191.

Payne B, Peters A. 1989. Cytochrome oxidase patches and Meynert cells in monkey visual cortex. Neuroscience 28:353–363.

Peters A. 1994. The organization of the primary visual cortex in the macaque. In: Peters A, Jones EG, editors. Cerebral cortex. New York: Plenum Press. p 1–31.

Purves D, LaMantia A. 1993. Development of blobs in the visual cortex of macaques. J Comp Neurol 334:169–175.

Rockland KS. 1992. Laminar distribution of neurons projecting from area V1 to V2 in macaque and squirrel monkeys. Cereb Cortex 2:38–47.

Rockland KS. 1997. Elements of cortical architecture: hierarchy revisited. In: Jones EG, Peters A, editors. Cerebral cortex, Volume 12, extrastriate cortex in primates. New York: Plenum Press. p 243–293.

Rockland KS, Virga A. 1990. Organization of individual cortical axons projecting from area V1 (area 17) to V2 (area 18) in the macaque monkey. Vis Neurosci 4:11–28.

Roe AW, Ts'o DY. 1997. The functional architecture of Area V2 in the macaque monkey. In: Rockland KS, Kaas JH, Peters A, editors. Cerebral cortex. New York: Plenum Press. p 295–333.

Sincich LC, Adams DL, Horton JC. 2003. Complete flatmounting of the macaque cerebral cortex. Vis Neurosci 20:663–686.

Sincich LC, Horton JC. 2002. Divided by cytochrome oxidase: a map of the projections from V1 to V2 in macaques. Science 295:1734–1737.

Sincich LC, Horton JC. 2003. Independent projection streams from macaque striate cortex to the second visual area and middle temporal area. J Neurosci 23:5684–5692.

Sincich LC, Horton JC. 2005a. Input to V2 thin stripes arises from V1 cytochrome oxidase patches. J Neurosci 25:10087–10093.

Sincich LC, Horton JC. 2005b. The circuitry of V1 and V2: integration of color, form, and motion. Annu Rev Neurosci 28:303–326.

Stepniewska I, Kaas JH. 1996. Topographic patterns of V2 cortical connections in macaque monkeys. J Comp Neurol 371:129–152.

Van Essen DC, Newsome WT, Maunsell JH, Bixby JL. 1986. The projections from striate cortex (V1) to areas V2 and V3 in the macaque monkey: asymmetries, areal boundaries, and patchy connections. J Comp Neurol 244:451–480.

Wong-Riley MTT. 1979. Changes in the visual system of monocularly sutured or enucleated cats demonstrable with cytochrome oxidase histochemistry. Brain Res 171:11–28.

Yabuta NH, Sawatari A, Callaway EM. 2001. Two functional channels from primary visual cortex to dorsal visual cortical areas. Science 292:297–300.